EURASIAN PHYSICAL TECHNICAL JOURNAL
2025, Volume 22, No.1 (51)
https://doi.org/10.31489/2025N1/127-133

Received: 28/10/2024 Revised: 26/02/2025 Accepted: 18/03/2025 Published online: 31/03/2025

Original Research Article

UDC 537.311.33(075)

PHOTOLUMINESCENCE SPECTRA OF DOPED N-TYPE INDIUM ANTIMONIDE CRYSTALS

Yegemberdiyeva S.Sh., Kushkimbayeva B.Zh., Kusherbayeva M.R.*, Keikimanova M.T.

M.Kh. Dulaty Taraz University, Taraz, Kazakhstan

*Corresponding authors: kmaikul@mail.ru

Abstract. *This paper presents a detailed study of photoluminescence of doped indium antimonide crystals. We have conducted a detailed study of photoluminescence of doped n-type indium antimonide crystals in a wide range of concentrations $1*10^{15}$ cm^{-3}-$1.5*10^{19}$ cm^{-3} at temperature 77 K. In this paper, we have for the first time obtained spectra of photoluminescence of indium antimonide with $n > 5*10^{17}$ cm^{-3} and experimentally discovered that spectrum of photoluminescence of indium antimonide with $n \geq 8.5*10^{16}$ cm^{-3} consists of two lines, maxima of which shift towards higher energies with increasing concentration. It has been established that shortwave line of doped n-type indium antimonide crystals' radiation is caused by recombination of electrons, located at Fermi level, with holes in valence band top. It has been shown that the best agreement between the experiment and theory in heavily doped crystals is reached by taking into account fluctuations of donor concentrations, dependence of the band gap on the degree of doping, as well as effective reduction of Fermi energy with increasing concentration.*

Keywords: photoluminescence of crystals, indium antimonide, Fermi level, doping, concentration, fluctuation, hole, band gap

1. Introduction

Indium antimonide (InSb) is a semiconductor with a narrow direct bandgap, $\Delta E_0 \approx 0.17$ eV at ambient conditions. Therefore, since its discovery in early fifties of twentieth century, InSb has naturally become one of the major choice materials for infrared (IR)-detecting devices [1].

Moreover, indium antimonide has long been considered a model semiconductor and it was indium antimonide on which the main theories created for crystals A^3 B^5 and their analogues (such as Kane's formalism) was tested. Interest in indium antimonide is caused not only by the peculiarities of its zone structure (narrow bandgap width, small effective mass of electrons, high mobility values), but also by the possibility to obtain single crystals in a very large concentration range (n- 10^{12}-$10^{19}$$cm^{-3}$; p - 10^{11}-10^{20} cm^{-3}). Although indium antimonide is a well-studied semiconductor, there is nevertheless very little work on photoluminescence studies. Of great scientific and often practical interest are studies of indium antimonide crystals containing initial concentrations of impurities, i.e., heavily doped crystals. When studying various physical effects in heavily doped n-type indium antimonide crystals, numerous anomalies have been found that are related not only to the degree of doping, but also to the grade (i.e., chemical nature) of doping impurity.

In recent years, scientists have been studying antimonide india according to various characteristics: Monnens, W., Billiet, N., Binnemans, K., et al. gives the following description: Indium antimonide (InSb) is

a III-V compound semiconductor with a narrow bandgap and a high electron mobility, and is used in various optoelectronic devices [2]. Electrodeposition represents a low-cost, scalable method for fabricating InSb films. In the literature, aqueous electrolytes and ionic liquids have commonly been applied. In this work, the electrodeposition of InSb films and nanowires from a dimethyl sulfoxide (DMSO)-based electrolyte was demonstrated. This electrolyte enabled electrodeposition in a broader potential range and at higher temperatures as compared to aqueous electrolytes. The electrolyte has a lower viscosity than ionic liquids, therefore exhibiting better mass transport properties for electrodeposition [2]. Muhammad Shafa, Sadaf Akbar, Lei Gao, Muhammad Fakhar-e-Alam & Zhiming M. Wang his work shows some important features of the growth of pure indium antimonide nanowires (InSb NWs) and their potential industrial applications [3]. Dilek Cakiroglu, Jean-Philippe Perez, Axel Evirgen and others from indium antimonide, photovoltaic cells were specially developed and manufactured for use in near-field thermophotovoltaic device demonstrators [4]. Therefore, indium antimonide, due to its specific properties, has long attracted the attention of researchers.

Unique properties of semiconductor quantum dots of the $A^3 B^5$ group are of particular interest due to high mobility of electrons, narrow band gap, and low effective mass of electrons. Manifestation of quantum size effects of such nanoclusters becomes possible even in the case of comparatively large sizes. Another advantage of narrow band gap and gapless semiconductors of the $A^3 B^5$ group is the possibility of synthesis on their basis of quantum dots with variable band gap and their further application in infrared (IR) and terahertz spectrum ranges. Nanoparticles, obtained by fine and ultrafine grinding of single-crystal plates and ingots of appropriate macro materials, are widely used in lasers [5, 6]. Besides this, development of technology to obtain $A^3 B^5$ compounds has shown that transition to creation of the large and very large integral circuits demands increasing diameter and improving structural perfection of single-crystals used as substrates [7, 8].

But of particular interest is the study of the photoluminescence spectra of n-type indium antimonide crystals. And the purpose of this work is to study the photoluminescence spectra of n-type indium antimonide doped crystals in the concentration range $2*10^{16}cm^{-3}$ - $4.8*10^{18}cm^{-3}$ at t=77K. Photoluminescence of indium antimonide is very weak and difficult to observe. There are few works on the study of photoluminescence of n-type indium antimonide crystals in the literature. They are mainly devoted to the study of crystals containing relatively small concentrations of electrons. In heavily doped indium antimonide crystals $n> 5*10^{17}cm^{-3}$ there appear “tails” of density of states in band gap, due to strong non-parabolicity of conduction band at $n \sim 10^{18}cm^{-3}$ the Fermi energy becomes of the order of band gap. Based on indium antimonide they produce sources of coherent radiation, photodetectors in wide spectral range. Besides this, InSb is used to make laser and tunnel diodes, infrared (IR) filters and magnetic field detectors [9].

Photoluminescence of indium antimonide was first investigated by Moss using optical excitation at room temperature in pure crystals. A relatively broad band with an emission maximum of 7-8 μm was detected. The author attributes this line to interzone recombination, since the position of the maximum of the emission spectrum approximately corresponds to the width of the forbidden zone of pure indium antimonide. Later, the emission of the p-n junction of indium antimonide was studied using electrical injection. In the study of photoluminescence of indium antimonide at 200 K, two intrinsic lines with emission maxima $hv_1 = 0.234eV$ and $hv_1 = 0.200eV$, and impurity lines $hv_1 = 0.216eV$ and $hv_1 = 0.230eV$ are observed.

2. Materials and research method

From the said above it is clear that most of the works on the study of photoluminescence of indium antimonide contain information related to pure crystals or to crystals alloyed to concentrations not exceeding $4.8*10^{17}$ cm^{-3}. Therefore, it is of high interest to carry out a detailed study of the photoluminescence of indium antimonide crystals with concentrations greater than $5*10^{17}$ cm^{-3}, especially crystals with $n > 10^{18}$ cm^{-3}. At such concentrations, several remarkable effects related to the degree of alloying and to the chemical nature of impurities were found. Strongly alloyed crystals of indium antimonide n-type display captivating value for the study of radiative processes also because of the already strong nonparabolicity of the conduction zone at $n \sim 10^{18}$ cm^{-3}, the Fermi energy becomes the order of the width of the forbidden zone (~0.22eV). It is also insightful that in strongly doped indium antimonide n-type crystals, the energy of plasma oscillations on the order of magnitude is close to the width of the forbidden zone.

Studied in detail photoluminescence spectra of n-type indium antimonide single crystals in a wide range (from $1.2*10^{15}cm^{-3}$ to $1.5*10^{19}cm^{-3}$) of carrier concentrations at liquid nitrogen temperature. In the literature

there are n-type indium antimonide photoluminescence spectra only for concentrations up to $n \leq 5*10^{17}cm^{-3}$. In the studied range of concentration, we have measured about 200 spectra of n-type indium antimonide photoluminescence [1]. Emission spectrum of indium antimonide with $n=5.4*10^{16}$ cm^{-3} consists of one line with maximum ħv=244 meV. The line width at half intensity is about 30 meV. The origin of this line was attributed to radiative direct transition of electrons from conduction band to valence band. Therefore, despite the widespread use of n-type indium antimonide, the luminescence spectra of doped crystals are not widely used, so this study is relevant . In this paper a new, not observed by authors [10,11] emission line appears in the long-wave part of the spectrum, in photoluminescence spectra of n-type indium antimonide, starting from $n \geq 8.5*10^{16}cm^{-3}$ electrons concentration. Thus, with an increase in the concentration of donor impurities, the main emission consists of two bands, maxima of which shift towards shorter wavelengths with increasing doping degree. Figure 1 shows the photoluminescence spectra of n-type indium antimonide for some of the studied crystals of different concentrations at a temperature of 77 K.

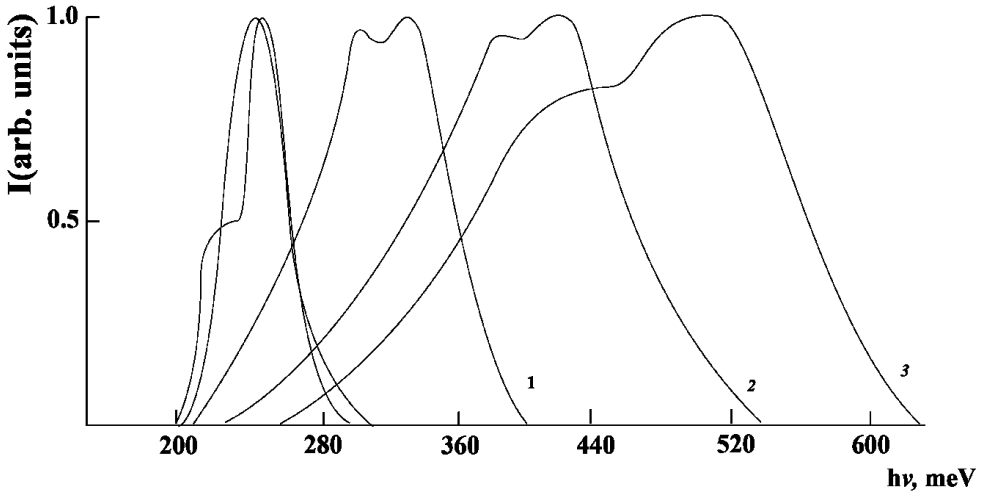

Fig.1. Photoluminescence spectra of indium antimonide at T=77 K and different concentrations, $1 - 9.8 \cdot 10^{17}cm^{-3}$, $2 - 2.8 \cdot 10^{18}cm^{-3}$, $3 - 4.8 \cdot 10^{18}cm^{-3}$

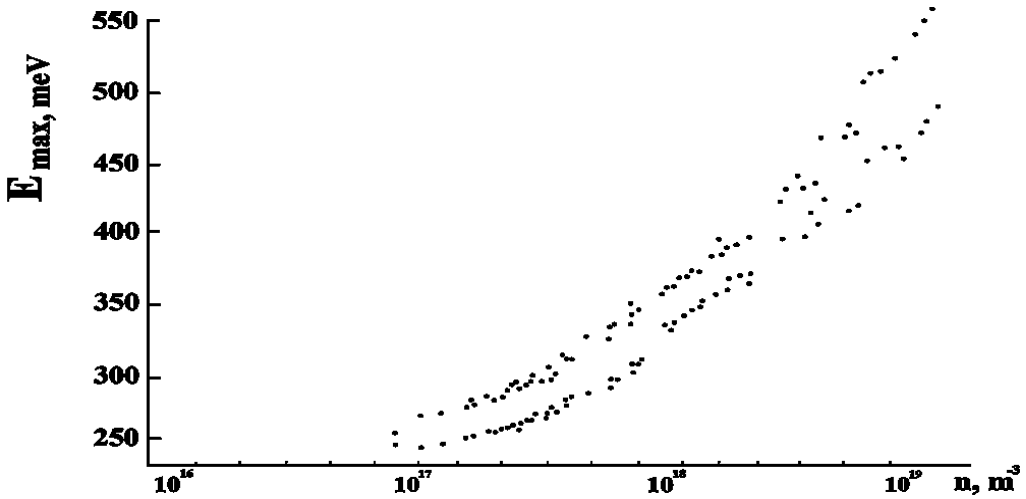

Fig. 2. Dependence of the energy position of the emission line maxima of indium antimonide crystals on the degree of doping

Figure 2 shows dependence of emission line maxima on doping level. From Figure 3 it can be seen that distance between two energy lines of emission remains approximately constant (30-40 meV) up to concentration $\sim 3*10^{18}cm^{-3}$, and then starts to increase, reaching ~80 meV at maximum concentrations. With

.

an increase of donor impurities concentration long-wave wing shifts towards higher spectrum energies. The integrated intensity of the emission line decreases with increasing electron concentration.

With increasing impurities concentration non-radiative recombination predominates, due to this the proportion of radiative recombination decreases, therefore the ratio of intensity of longwave and shortwave bands changes with increasing impurity concentration.

Experimental data can be explained taking into account features of the indium antimonide band structure: the spectrum of electrons in the conduction band is strongly non-parabolic, $m_e \ll m_{hh}$ (m_e- effective mass of electrons, m_{hh}- effective mass of heavy holes). If we assume that non-equilibrium holes have a lattice temperature and photoluminescence band is due to vertical transitions from conduction band to valence subbands, then the maximum of the band should be at an energy of the order of the band gap width ~E_g, which is not observed in the experiment. Another possibility may be in that effective temperature of non-equilibrium holes is significantly different from a lattice one and, as a result, there is a sufficient number of holes in the valence band with a wave vector equal to K_F (wave vector of electrons at Fermi level). In such a situation, the maximum of the emission band should be at a significantly higher photon energy than E_g (e.g. at n~10^{18}cm^{-3} Fig. 1 maximum should be at photon energy ~ $2E_g$, which roughly corresponds to experimental data for this concentration). However, for this we must assume that the effective temperature of the holes:

$$K\,T_h \sim \frac{\hbar^2 {K_F}^2}{2m_h} \sim E_g \frac{m_e}{m_h} \sim 25 мэВ, m_e\, T_h \sim 300\text{K} \quad (1)$$

We can describe a new shortwave part of the spectrum more exactly, if we suggest that it is caused by recombination of electrons, located at Fermi level, with holes at the top of the valence band, i.e. indirect transitions take place. The impulse in such a process is transferred from photoexcited holes to a charged donor. Mean free path of heavy holes l or inverse value $2\pi/l$, which determines impulse uncertainty can be estimated using Brooks-Herring formula scattering on charged impurities:

$$l = \frac{2}{\pi}\frac{\varepsilon^2 \mathcal{H}^2}{e^4 N_Д}\ \ \Phi(U) \quad (2)$$

where $\varepsilon -$ energy of a hole, $N_Д -$ concentration of charged impurities, $U = \frac{\Delta\varepsilon}{\varepsilon}$, $\Delta\varepsilon -$ energy transferred by impurity hole $\Phi(U) \approx lnU$. Substituting $\varepsilon \approx K_0T$, we shall obtain at $N_Д = 10^{19} cm^{-3}, l = 4 * 10^{-8} cm$ and then $\Delta K = \frac{2\pi}{l} = 1.5 * 10^7 cm^{-1}$. Thus, such processes ensure the transfer of impulse during indirect transition. Taking into account the non-parabolicity of the conduction band and neglecting the contribution of light holes, the expression for the relative intensity of optical transitions I can be written as

$$I = \sqrt{x}(1+x)^{\frac{3}{2}}(1+2x)\frac{1+x}{1+3x}\left(1+exp\frac{x-\frac{\varepsilon_F}{\varepsilon_g}}{\frac{K_0T}{\varepsilon_g}}\right)^{-1} \quad (3)$$

where $x = \frac{\hbar\omega_0 - \varepsilon_g}{\varepsilon_g}; \varepsilon_F -$ Fermi energy, $\varepsilon_g -$ band gap width, T-temperature, factor $\frac{1+x}{1+3x} -$ determines the dependence of the matrix element on energy; $\sqrt{x}(1+x)^{\frac{3}{2}}(1+2x)$ density of states in the conduction band $\left(1+exp\frac{x-\frac{\varepsilon_F}{\varepsilon_g}}{\frac{K_0T}{\varepsilon_g}}\right)^{-1} -$ Fermi electron energy distribution function. For non-parabolic conduction band ε_F is:

$$\varepsilon_F = \frac{\varepsilon_g}{2}\left[\left(1+\frac{\hbar^2 {K_F}^2}{m_c \frac{\varepsilon_g}{2}};\right)^{1/2} - 1\right] \quad {K_F}^2 = (3\pi^2)^{2/3} {n_D}^{2/3} \quad (4)$$

Figure 3 shows the results of calculation using formula (1) for some studied crystals. It is clear that up to concentrations ~2*10^{18}cm^{-3} this formula describes shortwave line of emission spectrum well enough.

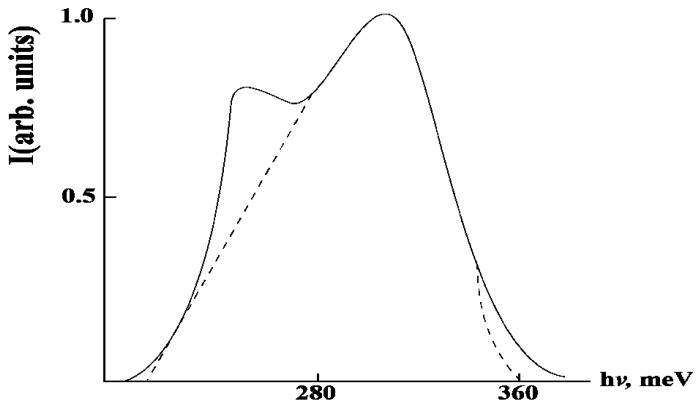

Fig. 3. Photoluminescence spectra of n-type indium antimonide 5.8*10^{17}cm^{-3} at T=77 K, where solid line - experiment, dotted line – theory

Figures show that with further increase in concentration of donor impurities in crystals (n>*10^{18}cm^{-3}) there is a lag observed between experimental maximum and theoretically calculated. This lag is growing with concentration increase, reaching ~100 meV at n=1.3*10^{19}cm^{-3}. This lag can be explained within the framework of a model, similar to the one used in paper to describe features of light absorption in heavily doped germanium.

The reason for the lag in energy of the experimentally observed short-wave peak from the theoretical prediction is that photoexcited holes are predominantly bound to fluctuations of impurities, which leads to a lag in the emission maximum from the position of the Fermi level.

Fluctuations in donor concentration lead to the formation of bound hole states. Such fluctuations will bind predominantly heavy holes. Let us estimate a value of U potential, caused by heterogeneity of donor distribution: $U = e^2 z/Lx$, L – radius of Thomas-Fermi screening, x – dielectric constant (permittivity), z – deviation of the number of donors from the average. $z = \sqrt{4/3\pi L^3 n}$. Then $U = (\frac{4}{3}\pi L e^4/x^2)^{1/2}$. For a degenerate electron gas $L = (\varepsilon_F x/6\pi e^2)^{1/2}$, where ε_F is calculated with regard to non-parabolicity of the conduction band. Characteristic wave vector of holes $k_{h,e}$ - in such potential is $k_{h,e} = (2m_h, eV/h^2)^{1/2}$ where $m_{h,e}$ – effective mass of heavy (light) holes. For $n = 3 \times 10^{18} cm^{-3}$, at $E_g = 0.22\ eV$, $E_F/E_g = 1.1$, $U = 25\ meV$, $k_F = (3\pi^2 n)^{1/3} \approx 4.5 \times 10^6 cm^{-1}$, $k_h = 5.5 \times 10^6 cm^{-1}$, $k_e = 1 \times 10^6 cm^{-1}$ [12].

These estimates show that maximum may shift towards long-wave side by value of $\sim 25\ meV$ and confirm an assumption that optical transitions into the area of heavy holes are indirect. Figure 4 schematically shows the indium antimonide band structure, position of Fermi level for $n = 3 \times 10^{18} cm^{-3}$ and optical transitions.

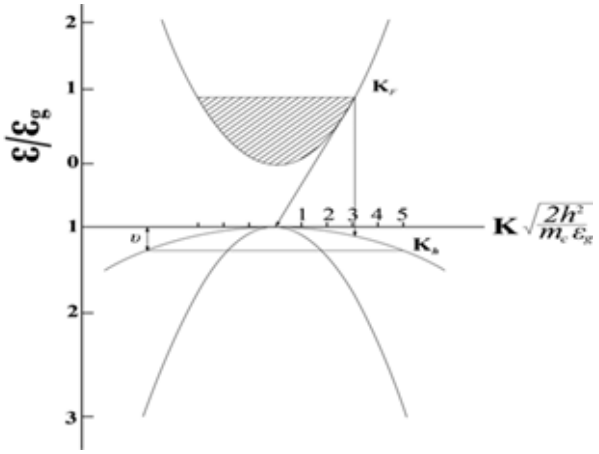

Fig.4. Zone scheme for crystal $n = 3 \times 10^{18} cm^{-3}$

.

Long-wave maximum may be caused by direct electrons transitions into the area of light holes. Presence of such transitions in indium antimonide absorption spectra was noted in the works. As it is clear from estimate, the root-mean-square fluctuation of the number of donors does not provide the necessary impulse of light holes, i.e. $k_e < k_F$. With increase in concentration of U value donors, $k_{h,e}$ increase. Experimentally this should lead to increased lag of short-wave band maximum position from theoretically calculated by (1) and its blurring which is observed experimentally .

3. Results and discussion

Taking into account changes of Fermi energy with increasing concentration shifts the theoretically calculated spectrum towards higher wavelengths, i.e. improves agreement between the experiment and theory.

From the above we can conclude that to explain shortwave radiation line in doped indium antimonide crystals it is necessary to consider all causes that lead to shifting radiation lines towards long-wave area:

a) fluctuations of donor's concentration;

b) floating of holes;

c) dependence of band gap width on doping degree;

d) effective reduction of Fermi energy in heavily doped crystals.

1. Conducted detailed study of photoluminescence spectra of doped indium antimonide crystals in ($1*10^{15}cm^{-3} – 1.5*10^{19}cm^{-3}$) interval of electrons concentration at 77K temperature.

2. In detail obtained spectra of indium antimonide crystals' photoluminescence with n $>5*10^{17}cm^{-3}$ concentrations. For the first time, experimentally discovered that the main radiation of n-type indium antimonide crystals with n > $8.5*10^{16}$ cm^{-3} concentrations consist of two lines.

3. It is shown that high-energy doped indium antimonide crystals radiation line is well explained by electrons recombination at Fermi level with holes at valence band top up to $\sim 2 * 10^{18}$ cm^{-3} concentrations.

4. It is established that to explain behaviour of shortwave indium antimonide crystals radiation line with n>$2*10^{18}cm^{-3}$ it is necessary to consider fluctuations of donor's concentration, dependence of band gap width on doping degree, as well as effective reduction of Fermi energy with increasing concentration

5. It is established that the shift of long-wave edge of radiation towards higher energy with increasing concentration is explained by the influence of impurity concentration fluctuations.

4. Conclusion

As already mentioned above, the long-wave wing of radiation spectrum of doped n-type indium antimonide crystals with increasing concentration shifts towards higher energy. This effect can be explained within the framework of a model, which we used to explain the shift of short-wave radiation line towards long waves, i.e. the model of optimal fluctuation of donor's concentration. We see that long-wave wing of radiation should shift towards higher energy with increasing concentration by value U_0. It should be noted that in crystals with n>$4*10^{18}cm^{-3}$ it is very difficult to precisely determine the position of long-wave edge of radiation (radiation was registered at the limit of resolution of the equipment used).

The physical causes of long-wave radiation line of doped indium antimonide crystals cannot be direct optical transitions into the light holes zone, as in this case its spectral position would not depend on impurities concentration. The dependence of impurity concentration, difference in energy positions of short-wave and long-wave maxima of the band does not allow to consider long-wave peak a background repetition of short-wave one. It is possible that long-wave line is caused by recombination of electrons, bound on the surface, as the above concentration dependences do not contradict such interpretation.

Conflict of interest statement

The authors declare that they have no conflict of interest in relation to this research, whether financial, personal, authorship or otherwise, that could affect the research and its results presented in this paper.

CRediT author statement

Yegemberdiyeva S.Sh.: Development of Facility and Measurements, Writing - Original Draft; Kushkimbayeva B.Zh.: Review & Editing; Keikimanova M.T.: Conceptualization, Data Curation; Kusherbayeva M.R.: Methodology, Investigation. The final manuscript was read and approved by all authors.

References

1 Palasyuk T., Jastrzebski C., Khachapuridze A., Litwin-Staszewska E., Suski T., Grzegory I., Porowski S. (2024) Influence of pressure on phonon properties of indium antimonide. *Physica Status Solidi (RRL) – Rapid Research Letters, 18*(9), 54-59. https://doi.org/10.1002/pssr.202400093

2 Monnens W., Billiet N., Binnemans K., et al. (2024) Electrodeposition of indium antimonide (InSb) from dimethyl sulfoxide-based electrolytes. *Journal of Solid State Electrochemistry, 28*, 3755–3768. https://doi.org/10.1007/s10008-024-05947-x

3 Shafa M., Akbar S., Gao L., et al. (2016) Indium antimonide nanowires: Synthesis and properties. *Nanoscale Research Letters, 11*, 164. https://doi.org/10.1186/s11671-016-1370-4

4 Cakiroglu D., Perez J.-P., Evirgen A., Lucchesi C., Pierre-Olivier C., Taliercio T., Tournié E., Vaillon R. (2019) Indium antimonide photovoltaic cells for near-field thermophotovoltaics. *Solar Energy Materials and Solar Cells, 203*. https://doi.org/10.1016/j.solmat.2019.110190

5 Tsvetkova O.Yu., Shtykov S.N., Zhukov D.N., Smirnova T.D. (2021) Synthesis and study of some properties of colloidal quantum dots of indium antimonide. *Izvestiya of Saratov University. Chemistry. Biology. Ecology, 21*(4), 378-381. https://doi.org/10.18500/1816-9775-2021-21-4-378-381 [in Russian]

6 Ledentsov N.N., Lott D.A. (2011) A new generation of vertical-emitting lasers as a key element of the computer communication era. *Advances in Physical Sciences, 181*(8), 884–890.

7 Kozlov R.Yu., Kormilitsina S.S., Molodtsova E.V., Zhuravlev E.O. (2021) Growing indium antimonide single crystals with a diameter of 100 mm by the modified Chochralsky method. *Izvestiya Vysshikh Uchebnykh Zavedenii. Materialy Elektronnoi Tekhniki = Materials of Electronics Engineering, 24*(3), 190-198. https://doi.org/10.17073/1609-3577-2021-3-190-198 [in Russian]

8 Averkiev N.S., Egemberdieva S.Sh., Kalinin B.N., Konstantinov O.V., Rogachev A.A., Filipchenko A.S. (1985) Photoluminescence of highly alloyed crystals of nn-type indium-antimonide. *Pisma v Zhurnal Tekhnicheskoi Fiziki*, 1326–1330. Available to: https://www.mathnet.ru/rus/pjtf1046

9 Komkov O.S., Firsov D.D., Lvova T.V., Sedova I.V., Semenov V.A., Soloviev A.N., Ivanov S.V. (2016) Photoreflection of indium antimonide. *Physics of the Solid State, 58*(12), 2394–2400. https://doi.org/10.1134/S1063783416120106

10 Velichko A.A., Ilushin V.A. (1993) Electrophysical properties of indium antimonide films obtained by molecular beam epitaxy. *Electronic Industry, 8*, 48-50.

11 Titkov A. N., Chaikina E.I., Komova E.M., Ermakova N.T. (1981) Low-temperature luminescence of degenerate p-type direct-bandgap semiconductors. *FTP (Semiconductors Physics and Technology, 15*(2), 345-352. [in Russian]

12 Allen L.P., Flint P.J., Meschew G., Dallas G., Bakken D., Brown G.J., Khoshakhlagh A., Hill C. J. (2011) 100mm diameter GaSb substrates with extended IR wavelength for advanced space-based applications. *SPIE Proceedings: Infrared Technology and Applications XXXVII, 8012*, 801215. https://doi.org/10.1117/12.882937

AUTHORS' INFORMATION

Yegemberdiyeva, Sofia Shaimerdenovna – Candidate of Physical and Mathematical Sciences, Associate Professor, Department of Physics and Informatics, Taraz University named after M.H. Dulati, Taraz, Kazakhstan; ORCID iD: 0009-0005-2418-2544; s.egemberdieva@bk.ru

Kushkimbayeva, Bibara Zhailaubaevna – Candidate of Physical and Mathematical Sciences, Associate Professor, Department of Physics and Informatics, Taraz University named after M.H. Dulati, Taraz, Kazakhstan; ORCID iD: 0000-0003-0572-0800; k.bibara@mail.ru

Kusherbayeva, Maikul Rakhmanberdievna – Master (Sci.), Senior Lecturer, Department of Physics and Informatics, Taraz University named after M.H. Dulati, Taraz, Kazakhstan; ORCID iD: 0000-0002-6707-7905; k.maikul@mail.ru

Keikimanova, Meruyert Tursynkhanovna – Candidate of technical sciences, Associate Professor, Department of Physics and Informatics, Taraz University named after M.H. Dulati, Taraz, Kazakhstan; ORCID iD: 0009-0006-1566-897x; merukey1970@mail.ru

.